

# Self-supervised signal denoising in magnetic particle imaging

Huiling Peng<sup>1,2,3</sup>, Jie Tian<sup>1,2,4,5</sup>, and Hui Hui<sup>1,2,3\*</sup>

<sup>1</sup> CAS Key laboratory of Molecular Imaging, Institute of Automation, Beijing 100190, China

<sup>2</sup> Beijing Key Laboratory of Molecular Imaging, Beijing 100190, China

<sup>3</sup> School of Artificial Intelligence, University of Chinese Academy of Sciences, Beijing 100190, China

<sup>4</sup> Key Laboratory of Big Data-Based Precision Medicine (Beihang University), Ministry of Industry and Information Technology of the People's Republic of China, Beijing, 100191, People's Republic of China

<sup>5</sup> Zhuhai Precision Medical Center, Zhuhai People's Hospital, affiliated with Jinan University, Zhuhai 519000, China

\* Corresponding author, email: hui.hui@ia.ac.cn

**Abstract:** Various noises restrict magnetic particle imaging (MPI) to achieve higher resolution and sensitivity in practice. In this study, we proposed a self-supervised learning method to denoise MPI signals. The deep learning-based architecture consisted with four encoder's blocks (EcBs) and four decoder's blocks (DcBs). This model was trained with limited data of MPI magnetization signals to efficiently suppress noise related features by directly learning from the noisy signals. Simulated experiments showed that the self-supervised method could reduce the noise interference in MPI signals and eventually improve image quality.

© 2023 Hui Hui; licensee Infinite Science Publishing

This is an Open Access article distributed under the terms of the Creative Commons Attribution License (<http://creativecommons.org/licenses/by/4.0>), which permits unrestricted use, distribution, and reproduction in any medium, provided the original work is properly cited.

## I. Introduction

Magnetic particle imaging (MPI) signal is contaminated by various noises that originated from many sources [1], including the thermal noise of the receive coil, harmonic interference from the non-linear electronic components, etc. These factors reduce the signal-to-noise ratio of the measured particle signal and system matrix, which will eventually worse the reconstructed image quality both in x-space and system matrix algorithms.

Deep learning has shown its superior in denoising tasks to traditional methods [2, 3]. However, the common supervised denoisers required massive noisy-clean pairs and it would be a challenge in MPI. To overcome this limitation, we introduce a self-supervised network, which is commonly used in image denoising tasks [4, 5]. By utilizing the consistency of MPI signal and the randomness of noise in different periods, the approach achieves noise suppression by measuring the MPI signal of two periods  $[u_1, u_2]$ . The self-supervised network aims to minimize the following empirical risk:

$$\arg \min E_{u_1} E_{u_2 | u_1} L(f_\theta(u_1), u_2) \quad (1)$$

where  $f_\theta(\cdot)$  denotes the denoising method with parameter  $\theta$ .  $L$  is the loss function.

## II. Methods

### II.1. Neural Network Architecture

Fig. 1 shows an encoder-decoder network as a frame. The input MPI signal  $u$  is mapped to an  $C \times N$  feature map then processed by four encoder's blocks (EcBs) and four

decoder's blocks (DcBs). Each EcB sequentially connects a down-sampling layer, a dropout layer, a parametric rectified linear unit (PReLU), and three resblocks. The feature map obtained  $i^{th}$  resblock is:

$$F_i(X_{i-1}) = W_{i2} * \max(0, W_{i1} * X_{i-1} + B_{i1}) + X_{i-1} + B_{i2} \quad (2)$$

where  $W_{i1}, B_{i1}, W_{i2}, B_{i2}$  represent the filters and biases of two convolutional layers respectively.  $*$  denotes the convolution operation. And each DcB is consisted of and up-sampling layer, a concatenation operation, two convolution layers and a PReLU. The feature map is mapped to the signal space by an up-sampling layer.

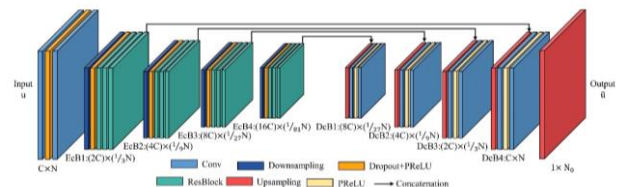


Figure 1: Architecture of designed self-supervised neural network. It is mainly composed of four encoder's blocks (EcBs) and four decoder's blocks (DcBs). The input to the network is the one periods MPI signal with the size  $1 \times N_0$ . Feature dimensions are described.

Considering that mean squared error loss leads to smoother results and limit noise suppression capabilities, mean absolute error is used as part of loss function:

$$L_{reg} = L_1(f_\theta(u_1), u_2) = \|f_\theta(u_1) - u_2\|_1 \quad (3)$$

In addition, we use prior knowledge of signals as the

regularization term to improve denoising performance. We utilized the special similarity in a scan period signal by matching the changing trend of the signal. We fine tune the learning direction of the network:

$$\lim_{\Delta t \rightarrow 0} \frac{u_{t+\Delta t} - u_t}{\Delta t} = \lim_{\Delta t \rightarrow 0} \frac{u_{T-t+\Delta t} - u_{T-t}}{\Delta t} \quad (4)$$

$$L_{GD} = \sum_{t \in (0, T/2]} u'_t - u'_{T-t} \quad (5)$$

Then, total various loss was added to improve signal smoothness:

$$L_{TV} = \sum_{t \in [0, T)} |u_{t+1} - u_t| \quad (6)$$

So the total loss function is:

$$L = L_{reg} + \alpha L_{GD} + \beta L_{TV} \quad (7)$$

where  $\alpha$  and  $\beta$  are the hyper-parameters.

## II.II. Numerical Experiments

To evaluate our method, we performed simulations based on two main MPI reconstruction methods: x-space reconstruction and system function reconstruction. The diameter of the magnetic nanoparticle is set to 30 nm. Magnetic field gradients of (0.4, 0.4) T/m/ $\mu_0$  were generated along (x, y) directions. In x-space reconstruction, we used Cartesian trajectory with frequencies 25 kHz and 0.5 kHz for scanning the field of view (FOV). In system function reconstruction, the Lissajous trajectory was used with frequencies 25kHz and 24.75kHz. The sampling frequency is 2.475MHz. The size of the FOV was set to  $101 \times 101$ .

For x-space reconstruction, we generate a dataset of 10000 MPI images with different particle distributions: 8000 images as the training set, 1000 images as the validation set, and 1000 images as the test set. The batch size, the learning rate,  $\alpha$ , and  $\beta$  are set to 4,  $1e-4$ , 0.05 and 0.01, respectively. For system function reconstruction, we obtain 10201 signal data using a simulated system matrix: 8160 data for training, 1020 data for validating, and 1021 for testing.

## II.III. Evaluation metrics and implementation

We verify the effectiveness of our method from the signals denoising results and the reconstructed image results. In terms of signals, signal-to-noise ratio (SNR) is used to evaluate the denoising ability of the method, root mean square error (RMSE) quantify the similarity of signals.

$$SNR = 10 \log_{10} \frac{\sum_{t=0}^T \tilde{u}(t)^2}{\sum_{t=0}^T (u(t) - \tilde{u}(t))^2} \quad (8)$$

$$RMSE = \sqrt{\frac{1}{T} \sum_{t=0}^T (u(t) - \tilde{u}(t))^2} \quad (9)$$

where  $u(t)$  and  $\tilde{u}(t)$  are denoised signal and clean signal, respectively.  $T$  means the length of the signal.

In terms of constructed images, we use peak signal to noise ratio (PSNR) and structure similarity index measure (SSIM) to evaluate the quality of image denoising and the similarity with the true value, respectively.

$$SSIM(X, Y) = \frac{(2\mu_X\mu_Y + c_1)(\sigma_{XY} + c_2)}{(\mu_X^2 + \mu_Y^2 + c_1)(\sigma_X^2 + \sigma_Y^2 + c_2)} \quad (10)$$

$$PSNR(X, Y) = 10 \log_{10} \frac{(max_X)^2}{\sum_{m=0}^M \sum_{n=0}^N (X(m, n) - Y(m, n))^2} \quad (11)$$

where  $X$  is the clean image and  $Y$  is the reconstructed image.  $\mu_X$ ,  $\mu_Y$ ,  $\sigma_X$  and  $\sigma_Y$  are the mean and standard deviation of image  $X$  and  $Y$ , respectively.  $\sigma_{XY}$  Is the covariance of  $X$  and  $Y$ .  $c_1$  and  $c_2$  are the constants set to 0.01 and 0.03.  $max_X$  means the maximum pixel value of image  $X$ .  $M$  and  $N$  indicate the rows and columns of the image.

## III. Results and discussion

### III.I Comparison

Table 1 summarizes the evaluation results of signal denoising for Gaussian noise with SNR=5dB and corresponding imaging quality after x-space reconstruction. And Table 2 shows the comparison results for Gaussian noise with SNR=15dB and harmonic interference with SIR=5dB. The comparison example of signal denoising and the reconstructed image using x-space algorithm is shown in Fig. 2. To evaluate the de-noising performance of the proposed framework, we compared it with two self-supervised denoisers: Noise2Noise (N2N) [4] and Recorrupted-to-Recorrupted (R2R) [6].

We evaluate the methods from the results of signal denoising and image reconstruction. The quantitative results are shown in Table 1. It can be seen that our method performs more adapted to MPI signal denoising tasks than other self-supervised methods. In addition, with the noise distribution becoming more complex, the performance of R2R drops rapidly, and our methods keep a stable state.

Table 1: Quantitative results of different methods for Gaussian noise with SNR=5dB.

	Signal Denoising		Reconstructed Image	
	SNR	RMSE	SSIM	PSNR
Noisy	5.00	128.27	0.39	21.13
N2N[4]	16.53	34.17	0.87	28.30
R2R[6]	11.68	60.50	0.69	24.90
Proposed	20.97	20.95	0.95	31.66

Table 2: Quantitative results of different methods for Gaussian noise with SNR=15dB and harmonic interference with SIR=5dB.

	Signal Denoising		Reconstructed Image	
	SNR	RMSE	SSIM	PSNR
Noisy	6.20	116.33	0.47	22.58
N2N[4]	17.48	30.92	0.89	29.06
R2R[6]	8.83	88.04	0.55	23.23
Proposed	22.72	16.59	0.94	31.46

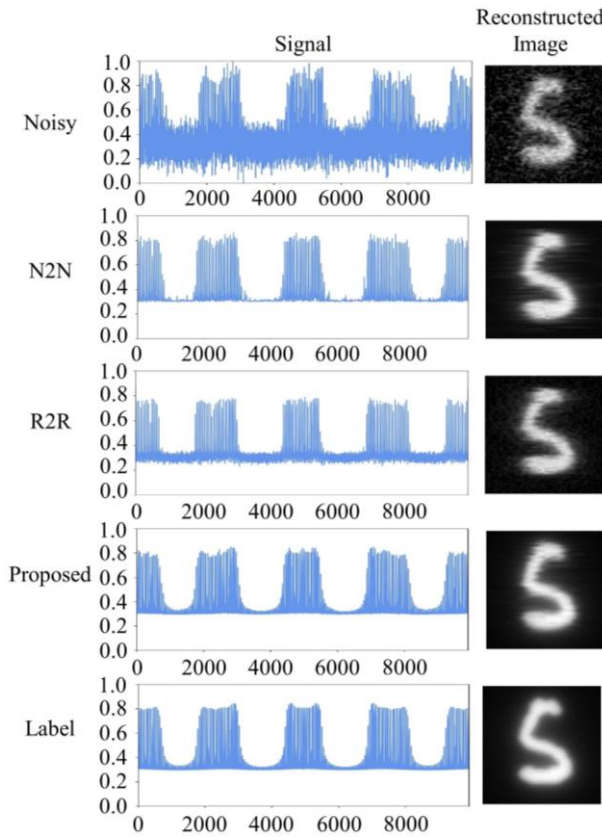


Figure 2: The comparison of denoised signal and the corresponding reconstructed  $x$ -space image.

Table 3 shows the denoising results on system matrix. The 3<sup>rd</sup> and 7<sup>th</sup> harmonic components of the system matrix before and after denoising is shown in Fig. 3. The harmonic data was reshape to  $101 \times 101$ , which same as the image size. It can be seen that the self-supervised method reduces the noise in system matrix. Even in high frequency where the proportion of noise component is higher, the method can still achieve noise suppressed.

Table 3: Quantitative results of proposed self-supervised network in system matrix reconstruction.

	Signal Denoising		Reconstructed Image	
	SNR	RMSE	SSIM	PSNR
Noisy	4.99	105.25	0.96	38.13
Proposed	19.17	20.61	0.99	43.90

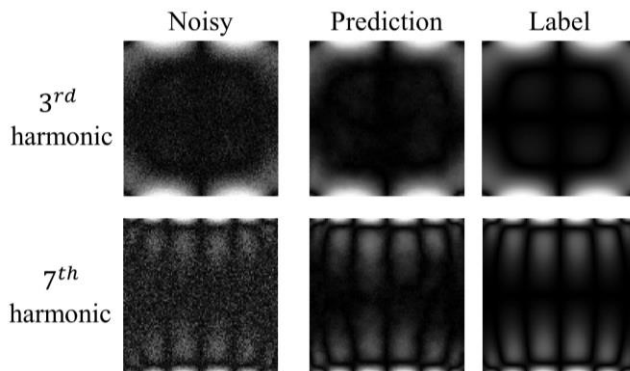


Figure 3: The visualization for two harmonic components.

## IV. Conclusions

In this work, we developed a self-supervised approach for denoising MPI signals for  $x$ -space and system matrix reconstructions. The proposed method minimizes the average deviation and uses the prior information of MPI signals, realizing the learning of signal pattern from noisy data. Our method shows that we can take the advantages of learning based method in denoising tasks while reduced the dependence on high quality MPI signal. Moreover, our method has the potential to alleviates the time consumption caused by multiple measurements of the system matrix.

## ACKNOWLEDGMENTS

The authors would like to acknowledge the instrumental and technical support of Multimodal Biomedical Imaging Experimental Platform, Institute of Automatic, Chinese Academy of Sciences. This work was supported in part by the National Key Research and Development Program of China under Grant: 2017YFA0700401; the National Natural Science Foundation of China under Grant: 62027901, 81827808, 81227901; Beijing Natural Science Foundation JQ22023; CAS Youth Innovation Promotion Association under Grant 2018167 and CAS Key Technology Talent Program.

## AUTHOR'S STATEMENT

Conflict of interest: Authors state no conflict of interest.

## REFERENCES

- [1] H. Paysen, O. Kosch, J. Wells, N. Loewa, and F. Wiekhorst, "Characterization of noise and background signals in a magnetic particle imaging system," (in English), *Physics in Medicine and Biology*, vol. 65, no. 23, Dec 7 2020.
- [2] P. Singh and G. Pradhan, "A New ECG Denoising Framework Using Generative Adversarial Network," (in English), *Ieee-Acm Transactions on Computational Biology and Bioinformatics*, vol. 18, no. 2, pp. 759-764, Mar-Apr 2021.
- [3] Y. X. Shang *et al.*, "Deep learning for improving the spatial resolution of magnetic particle imaging," (in English), *Physics in Medicine and Biology*, vol. 67, no. 12, Jun 21 2022.
- [4] J. Lehtinen *et al.*, "Noise2Noise: Learning Image Restoration without Clean Data," *International Conference on Machine Learning, Vol 80*, vol. 80, 2018.
- [5] N. Moran, D. Schmidt, Y. Zhong, and P. Coady, "Noisier2Noise: Learning to Denoise From Unpaired Noisy Data," in *2020 IEEE/CVF Conference on Computer Vision and Pattern Recognition (CVPR)*, 2020, pp. 12061-12069.
- [6] T. Y. Pang, H. Zheng, Y. H. Quan, and H. Ji, "Recorrupted-to-Reconstructed: Unsupervised Deep Learning for Image Denoising," (in English), *2021 Ieee/Cvf Conference on Computer Vision and Pattern Recognition, Cyp 2021*, pp. 2043-2052, 2021.